Neuron, Volume *88*

Supplemental Information

Internally Recurring Hippocampal Sequences as a Population Template of Spatiotemporal Information

Vincent Villette, Arnaud Malvache, Thomas Tressard, Nathalie Dupuy, and Rosa Cossart

Supplemental data

Figure S1. Related to Figures 1 and 2.
Figure S2. Related to Figure 1.
Figure S3. Related to Figures1 and 2.
Figure S4. Related to Figure 4.

Table S1. Related to Figures 2 and 4.

Movie S1. Related to Figure 1.

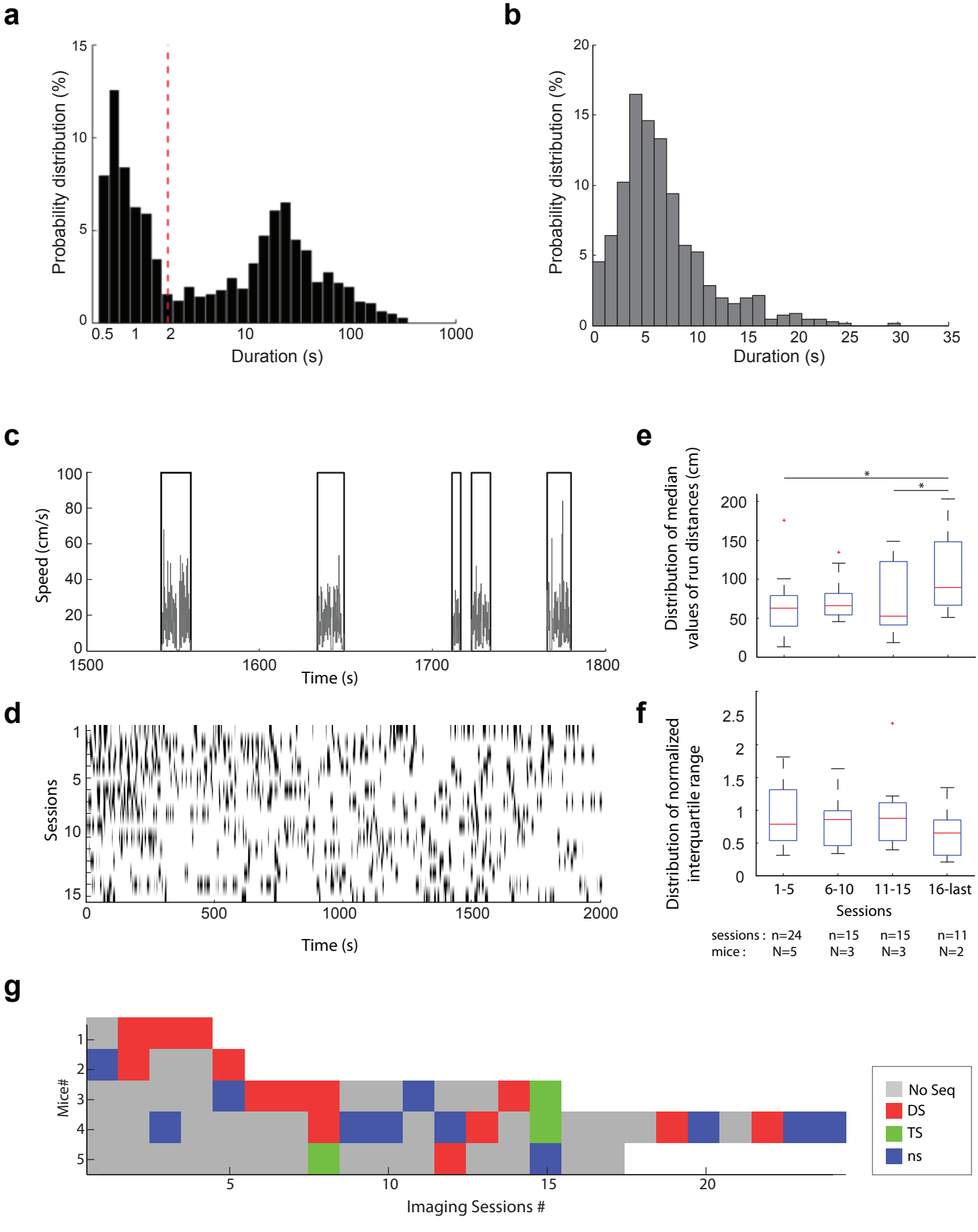
a
Probability distribution (%)
Duration (s)
b
Probability distribution (%)
Duration (s)
c
Speed (cm/s)
Time (s)
d
Sessions
Time (s)
e
Distribution of median values of run distances (cm)
f
Distribution of normalized interquartile range
1-5
6-10
11-15
16-last
Sessions
sessions : n=24 n=15 n=15 n=11
mice : N=5 N=3 N=3 N=2
g
Mice#
Imaging Sessions #
No Seq
DS
TS
ns

Figure S1. Behavioral features of dataset.

Distribution of spontaneous travel pauses (a) and run epochs durations (b). Pauses were automatically detected with a minimum threshold of 0.5s (n=5 mice). **a**. Note the log scale on the x axis. The travel pause durations segregated into two groups: short immobility periods (<2s, n=633) and rest epochs (>2s, n=762). **b**. Histogram represents the distribution of run epochs durations (median value: 6.3 s, n=5 mice, 1380 run epochs). **c**. Five consecutive run epochs (black rectangles) occurring within a 300 s time window, speed is indicated in gray. **d**. Illustration of 703 run epochs occurring across 15 sessions for the same mouse. **e-f**. Evolution of run distance per run epochs; imaging sessions were divided into 4 groups (1^{st} to 5^{th}, 6^{th} to 10^{th}, 11^{th} to 15^{th} and $>15^{th}$). Box plots indicate the distribution calculated for each session within each group of median values (e) and of normalized interquartile ranges (f). Two-sample Kolmogorov-Smirnov test: * $p<0.05$, ** $p<0.01$. Interquartile range was normalized to the median value in order to evaluate behavioral stereotypy. No statistically significant evolution was observed. **g**. Figure represents sequence occurrence across imaging sessions. We report two different conditions: (1) no sequence could be observed (gray); (2) recurring sequences could be detected: Distance-modulated sequences (red); time-modulated sequences (green); no preferential spatio-temporal modulation (blue).

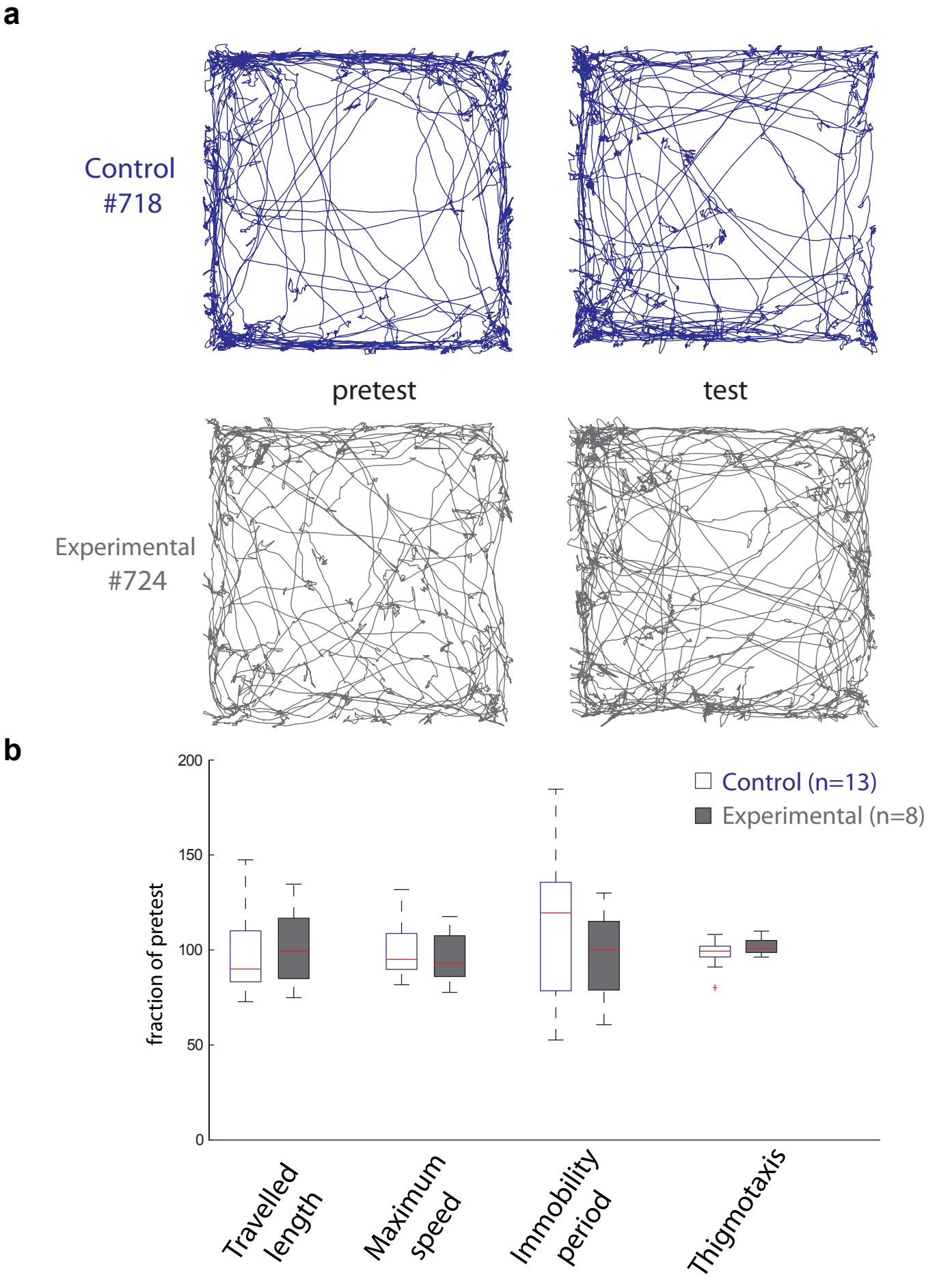
a
Control
#718
pretest
test
Experimental
#724
b
Control (n=13)
Experimental (n=8)
fraction of pretest
200
150
100
50
0
Travelled length
Maximum speed
Immobility period
Thigmotaxis

Figure S2. Analysis of mouse exploratory behavior before and after surgery.

a. Exploration tracks from two representative mice from the control (blue) and experimental (gray) group during pretest and test. **b**. Quantification of the behavioral parameters expressed as a fraction of the pretest for control (n=13, white boxplot) and experimental mice (n=8, gray). Data is represented in boxplots where the horizontal red line indicates the median and crosses indicate outliers.

Even if our protocol has been validated by previous publications [1,2], we examined the impact of the experimental procedure on exploratory activity using a classic open field test. Mice that were virally injected, water deprived for surgery, and implanted with a chronic hippocampal window with a head fixation bar were compared to control mice (experimental group: n=8, control group: n=13). Control mice, were sex-, littermate- and age- matched to the experimental ones. All animals were handled and weighted daily and exposed to the same light/dark cycle. Tests were performed in a sound-attenuated experimental room during the light period. A pretest was initially performed to remove inter-individual variability. Testing was performed 10 days after the surgery. The apparatus consisted of a dark blue plastic box (40 × 40 cm) with 30 cm-high walls. Each mouse was initially placed facing a corner and allowed to explore freely for 10 min. A video tracking system (Ethovision, Noldus) recorded the mouse trajectory (25Hz). A custom written routine (Matlab) was used to compute the following parameters per test session: the travelled distance, the maximum speed (mean of the last quartile of the sorted instantaneous speed), the immobility time period (fraction of time spent at a speed <1cm/s) and thigmotaxis (fraction of time spent along the walls, a commonly accepted index of anxiety [3]). Statistical comparisons were done using a two-sample Kolmogorov-Smirnov test. No significant difference in behavior was observed.

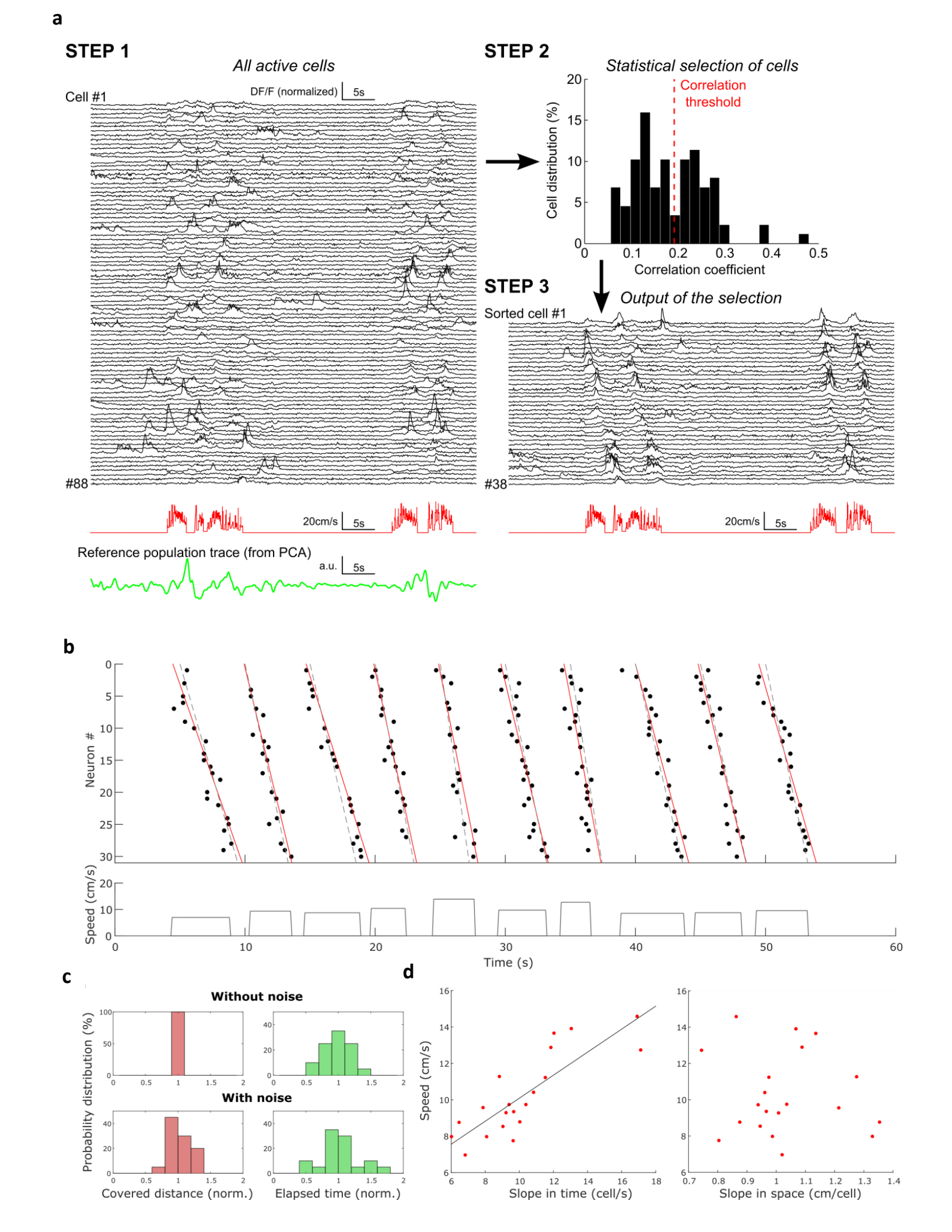
a
STEP 1
All active cells
Cell #1
DF/F (normalized)
5s
#88
20cm/s
5s
Reference population trace (from PCA)
a.u.
5s
STEP 2
Statistical selection of cells
Correlation threshold
Cell distribution (%)
Correlation coefficient
STEP 3
Output of the selection
Sorted cell #1
#38
20cm/s
5s
b
Neuron #
Speed (cm/s)
Time (s)
c
Without noise
With noise
Probability distribution (%)
Covered distance (norm.)
Elapsed time (norm.)
d
Speed (cm/s)
Slope in time (cell/s)
Slope in space (cm/cell)

Figure S3. **Detection and Simulation of recurring sequential neuronal activation**

a. Three Steps illustrate the detection of recurring sequential neuronal activation. Step 1: Fluorescence signals of 88 active cells in a 60s time window, with the corresponding mouse speed below (red) and the reference signal holding the highest information content about activity during run (green). Step 2: histogram shows the distribution of the correlation coefficients between the reference signal and the fluorescence traces of each active cell. Red dashed line indicates Otsu's threshold. Step 3: fluorescence signals of the cells thus detected as involved in recurring activity, sorted by their order in the sequence. **b-d**. Simulation of the detection of distance sequence in noisy data. **b**. Outcome of distance-sequence simulation: rasterplot of neuronal activation and speed as a function of time for 10 simulated sequences. Red line: fit of the noisy sequences, dashed gray line: theoretical slope (without noise). **c**. Histograms plotting the distributions of the simulated covered distances (red) and elapsed times (green) without and with noise (normalized to their median). The former distributions are statistically different (K-S test, p<0.01) whereas the latter are not. **d**. Speed vs temporal and spatial slope correlations on simulated data in the noisy case. As in the experimental data, the temporal slope (left) is statistically correlated (Spearman, p<0.001) to the speed of the animal.

To explicitly show the robustness of correlation analysis in noisy data, we have simulated distance sequences with and without variability and measurement errors. We did the following procedure:

For each cell i of the sequence j, we calculate its firing onset time using the following equation:

$$Onset(i) = \frac{i}{a\, v_j} + \varepsilon_c(i,j)$$

Where a is the spatial coding rate (in cell/cm), v_j is the median velocity of the animal during the sequence j and $\varepsilon_c(i,j)$ is a random noise that reproduces the cell temporal error.
To create a noisy dataset that mimics the experimental data, we added variability: 1) in cell participation (a given cell participates to 70% of the sequences); 2) in velocity $v_j = {v_j}^0\left(1 + \varepsilon_v(j)\right)$ to reproduce outliers (that could come from speed measurement errors and/or animal's speed estimation error).
For the simulation, we used a set of 30 cells and 20 sequences with a random velocity:
$STD\left({v_j}^0\right) = 2\ cm/s$, normal distribution, $MEAN\left({v_j}^0\right) = 10\ cm/s$
The simulation was performed using the following errors:
$STD(\varepsilon_c) = 0.4\ s$, normal distribution
$STD(\varepsilon_v) = 0.1$, uniform distribution
The spatial coding rate was $a = 1\ cell/cm$ thus the distance unit was set to 30 cm.

We generated 1000 sets of DS, an example of which is plotted on Figure S3b. We first compared the surrogate distributions of elapsed time and traveled distance (Figure S3c): there was always a statistical difference in the case without noise (p<0.05 in 100% of cases, Kolmogorov-Smirnoff test) however the difference was no longer significant when noise was added (p<0.05 in 0.2% of cases). Using the same type of analysis as performed with our experimental data in the noisy case, we found a distance correlation (p<0.05 in 98% of cases) and no time correlation (p<0.05 in 4.3% of cases); the estimated distance unit was 30.3 +/- 1.3cm (Figure S3d). As a conclusion this simulation clearly illustrates how our method is suited for noisy data whereas an intuitive one-dimensional analysis is not.

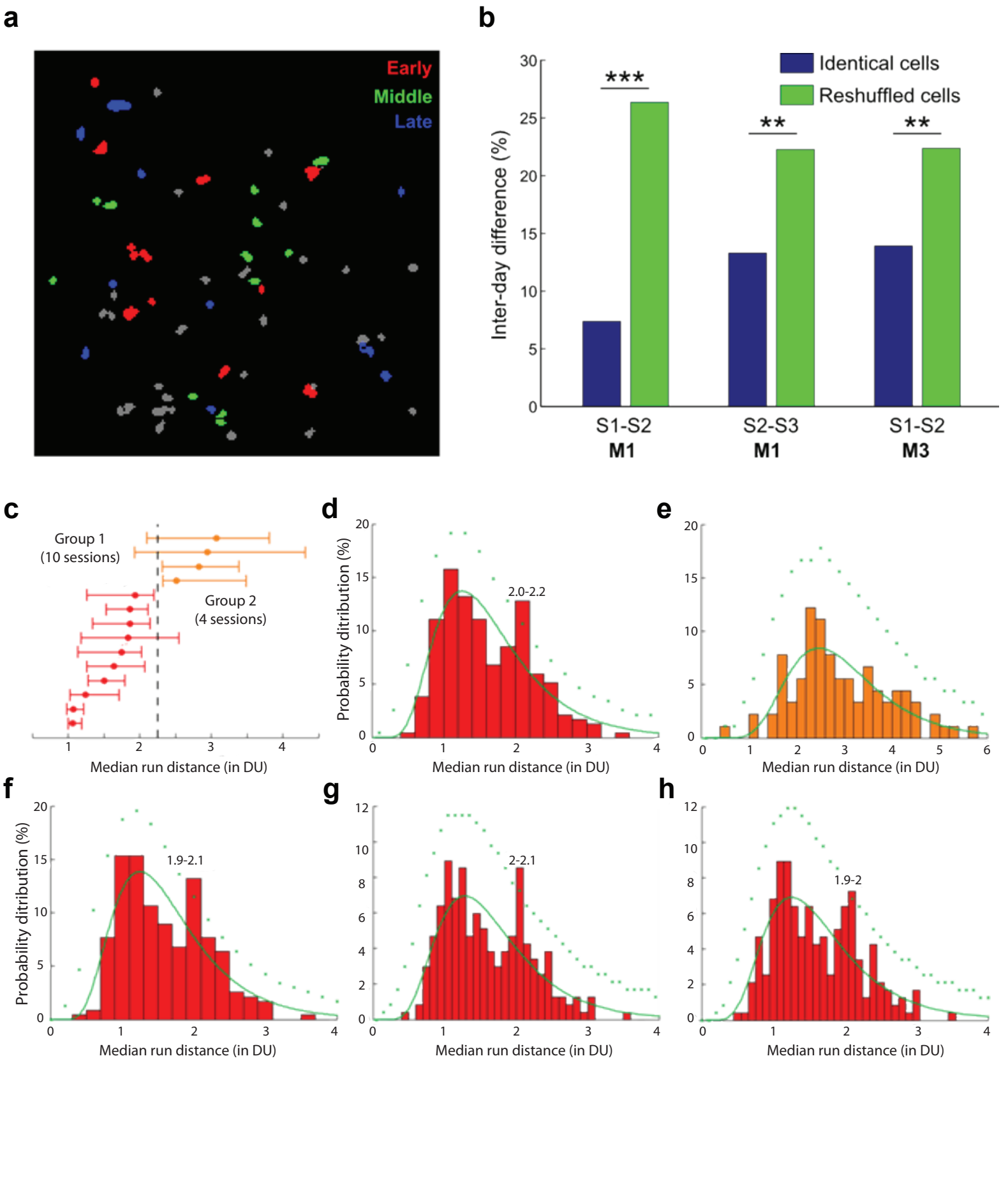
a
Early
Middle
Late
b
Identical cells
Reshuffled cells
Inter-day difference (%)
***
**
**
S1-S2
M1
S2-S3
M1
S1-S2
M3
c
Group 1
(10 sessions)
Group 2
(4 sessions)
Median run distance (in DU)
d
Probability ditribution (%)
2.0-2.2
Median run distance (in DU)
e
Median run distance (in DU)
f
Probability ditribution (%)
1.9-2.1
Median run distance (in DU)
g
2-2.1
Median run distance (in DU)
h
1.9-2
Median run distance (in DU)

Figure S4. Multiple features of DS.

a. Representative map of the spatial arrangement of the cells according to their activation order within a DS. No significant spatial organization of neurons involved in DS could be detected. Contours of the cells active within the first third of the DS are filled in red, second third in green and last third in blue. Gray filled contours indicate active neurons that do not participate in DS. To test whether the neurons involved in DS were more spatially clustered than expected by chance we calculated the median pairwise distance between cells in DS and compared this value to that obtained with cell reshuffling. Over the 14 sessions with DS, no significant clustering was observed ($p=0.3$ using the cumulative distribution over 1000 reshufflings). To investigate if there was a link between the sequence dynamics and the DS map in CA1, we divided the DS in three cell groups with respect to their median firing time in the DS. No significant clustering could be observed either ($p>0.05$ using the cumulative distribution over 1000 reshufflings). **b**. Histogram representing the statistical evaluation of the sequence repetition across days. For each pair of DS cells, we calculated the variation from one day to the next of the distance traveled between their activation onsets, normalized to the "distance unit" of the DS (inter-day difference). The same calculation was performed on a random set of cells involved in the DS (same number of cells). The median value of the inter-day difference is displayed on the figure. In blue: cells recruited on both days; in green: the random set of cells. ** $p<0.01$; *** $p<0.001$ (K-S test). For mouse 1 (M1), the three imaging sessions S1, S2 and S3 were done on consecutive days; For mouse 3 (M3), the two imaging sessions S1 and S2 were done on consecutive days. **c-h**. Bimodal distribution of median run distance expressed in DU. **c**. Distribution (median and inter-quartile range) of normalized run distance (to the DU) for each session (sorted using median value). **d-e**. Distributions of normalized run distances of the two groups of imaging sessions outlined in c. Group 1 (d, red): median smaller than 2; Group 2 (e, orange): median greater than 2.5; Green line: log-normal fit, Green crosses: significance curve ($p<0.05$) for each peak (see methods). **f-h**, the significant peak of the first group was robust against different binning phases (f) and sizes (g,h).

		Distance Test		Time Test		Cell count	Sequence count	D. unit (cm)	Speed (cm/s)	Run epoch (in D. unit)
		ρd	p-val	ρt	p-val					
M1	S1#	0.38	*	0.04	n.s.	36	57	18	8.0	3.1
	S2#	0.75	***	0.03	n.s.	31	72	28	10.4	2.5
	S3#	0.56	*	-0.08	n.s.	38	31	12	6.8	2.9
M2	S1	0.73	***	-0.31	n.s.	30	42	51	10.6	1.5
	S2	0.61	*	0.14	n.s.	32	34	39	10.1	1.2
M3	S1#	0.53	**	-0.22	n.s.	22	30	47	12.2	1.8
	S2#	0.51	*	-0.08	n.s.	32	20	61	12.8	1.9
	S3	0.68	**	0.01	n.s.	22	32	44	13.1	1.7
	S4	0.44	**	0.25	n.s.	40	49	21	6.6	2.8
M4	S1	0.54	*	0.30	n.s.	52	22	87	11.9	1.1
	S2	0.61	*	0.08	n.s.	65	24	113	10.1	1.1
	S3	0.83	***	-0.22	n.s.	54	21	74	10.0	1.9
	S4	0.58	**	-0.23	n.s.	57	31	77	11.2	1.9
M5	S1	0.59	*	0.40	n.s.	29	28	55	13.2	1.6

Table S1. Detailed dataset for the 5 mice (M1 to M5) and the 14 sessions where DS could be imaged (#: same field of view on consecutive days).

Coefficients (ρ) and their corresponding significance (p-val: n.s. $p>0.05$, * $p<0.05$, ** $p<0.01$ and *** $p<0.001$) for the Spearman correlation between temporal slopes and speed (Distance test, ρd) and between spatial slopes and speed (Time test, ρt); Cell count: absolute number of cells involved in DS; Sequence count: absolute number of sequences during the session; D. unit: median ”distance unit” over all the DS within an imaging session; Speed: median speed across all run epochs of the imaging session; Run epoch: median distance traveled during the run epochs expressed relative to the corresponding “distance unit”.

Movie S1.

Left panel: Movie of the GCaMP5G fluorescence signal imaged in the CA1 stratum pyramidale of a mouse running in the dark on a treadmill without cues. Right panel: Fluorescence traces from three neurons in the movie involved in recurrent sequences of neuronal firing as the mouse spontaneously travels on the treadmill. Bottom graph indicates mouse speed.

Supplemental references

[1] D. A. Dombeck*, et al.*, "Functional imaging of hippocampal place cells at cellular resolution during virtual navigation," Nat. Neurosci. **13**(11), 1433 (2010).

[2] M. Lovett-Barron*, et al.*, "Dendritic inhibition in the hippocampus supports fear learning," Science **343**(6173), 857 (2014).

[3] P. Simon, R. Dupuis, and J. Costentin, "Thigmotaxis as an index of anxiety in mice. Influence of dopaminergic transmissions," Behav. Brain Res. **61**(1), 59 (1994).